Supplementary Information

Peak-fitting assisted SERS strategy for accurate discrimination of carboxylic acid enantiomers

Jing Tao, Dan Li, * Yanyan Guo and Wei Deng

College of Chemistry and Environmental Engineering, Shanghai Institute of Technology, Shanghai 201418, P. R. China, E-mail: dany@sit.edu.cn

*To whom the correspondence should be addressed. E-mails: dany@sit.edu.cn

Experimental section

Materials. Chloroauric acid ($HAuCl_4 \cdot 4H_2O$，99.9%), cetyl trimethyl ammonium bromide (CTAB, ≥99%), sodium citrate ($Na_3C_6H_5O_7 \cdot 2H_2O$, 99.9%), sodium boron hydride ($NaBH_4$, 99%), silver nitrite ($AgNO_3$, ≥99.9%), hydrochloric acid (HCl 37%), L(+)-Ascorbic acid ($C_6H_8O_6$, 99%), D-(+)-Glucose ($C_6H_{12}O_6$), L-(-)-Glucose ($C_6H_{12}O_6$, 98%), (R)-2-Chloropropionic Acid ($C_3H_5ClO_2$, ≥98%), (S)-(-)-2-Chloropropionic acid ($C_3H_5ClO_2$) and 4-mercaptophenylboronic acid ($C_6H_7BO_2S$, 90%) were purchased from Titan-Reagent (Shanghai, China). Deionized water with a conductivity of 18.1 MΩ cm was used throughout this work.

Synthesis of GNRs@MPBA. GNRs was prepared via sodium borohydride seeding growth protocol. [1] First, Au seed solution was prepared by adding 0.6 mL of 0.01 M precooled $NaBH_4$ solution to the mixture of 10 mL of 0.1 M CTAB and 1 mL of 0.01 M $HAuCl_4$. The seed solution was aged for 2 h at the room temperature after the color of the reaction system changed to brown. Next, the solutions were mixed under continuously stirring in the following order: 40 mL of 0.1 M CTAB solution, 0.4 mL of fresh 0.01 M $AgNO_3$ solution, 0.8 mL of 0.01 M $HAuCl_4$ solution, and 320 μL of 0.1 M fresh ascorbic acid aqueous solution. Finally, 50 μL of the as-prepared Au seed solution was added, and the reactants were kept undisturbed for 6 h at the room temperature. After the reaction, GNRs were obtained by centrifuging and repeatedly washing with water. Then 0.5 mL of 1 mM MPBA was added into 5 mL of purified GNRs solution. The mixture was incubated at 30 °C for 24 h. Excess MPBA was removed by centrifugation at 8,000 rpm for 5 min and dispersed in deionized water. By using ICP-MS measurements we estimated average 126 MPBA on each GNRs. The resultant MPBA-modified GNRs (GNRs@MPBA, 0.85 nM) were kept at 4 °C before use, whose concentrations were estimated by Lambert-Beer Law. [2]

Synthesis of GNRs@MPBA-D(Glu), GNRs@MPBA-L(Glu), and GNRs@MPBA-DL(Glu). The synthesis of chiral GNRs@MPBA-Glu is schematically shown in Scheme S1A. Initially, 0.018 g of L(Glu) powders were soaked into 10 mL of GNRs@MPBA (0.85 nM) buffer solution (pH~9.0). The mixture was incubated at room temperature for 24 h. Excess L(Glu) in the mixture was removed by centrifugation at 8,000 rpm for 10 min. Afterward, the precipitates were washed with methanol for 2-3 times. Finally, the resulting GNRs@MPBA-L(Glu) (0.8 nM) was dispersed in deionized water for use. By replacing L-Glu with D- or DL-Glu, GNRs@MPBA-

D(Glu) and GNRs@MPBA-DL(Glu) substrates were also prepared using the same procedure above.

Characterizations. TEM images were obtained on the FEI TECNAI G2-F20. ^{1}H NMR spectra were collected on a AVANCE III 500MHz equipment. The chemical shifts were recorded in ppm relative to DMSO and with the solvent resonance as the internal standard. Electronic circular dichroism (CD) and UV-vis absorption spectra were acquired on the JASCO-820 spectropolarimeter with a DRCD-466L unit (DRCD: Solid-state diffuse reflectance circular dichroism).

SERS spectra were recorded on a Renishaw Invia Micro-Raman system equipped with a 785 nm laser. For Raman measurements, an integration time of 8 s was chosen and the spectrum was collected with a laser power of 10 mW. The baseline-corrected spectra were normalized with respect to the peak at 1078 cm^{-1} for 4-MPBA-modified samples. To assess the Raman enantio-discrimination ability of GNRs@MPBA-Glu, three kinds of chiral molecules were selected, which included 2-chloropropionic acid (CPA), lactic acid (LA) and β-hydroxybutyric acid (HBA) (their molecular structures are shown in Scheme S1B). And the sample treatments before Raman measurements are conducted as follows: 1) about 0.25 mL of GNRs@MPBA-Glu (0.8 nM) with a given handedness tag (D-, L-, or DL-) were mixed with 0.2 mL of a specific enantiomer solution with a given concentration; 2) after 24 h incubation, the above mixture was dropped on a silica substrate and dried in air for the following Raman test.

DFT calculations. All DFT calculations were performed with latest version of ORCA quantum chemistry software (Version 5.0.1).[3] The corrected version of B97 exchange-correlation functional proposed by Grimme (so-called B97-3c) was adopted for all calculations.[4] The ground-state geometries were fully optimized at the DFT level of theory using the B97-3c functional. [5] The B97-3c functional utilized three corrections: the D3BJ method including three-body term to account for long-range dispersion interactions,[6] a short-range bond-length correction (SRB) which corrects for systematically overestimated covalent bond-lengths and electronegative elements, and a modified stripped-down triple-ζ basis (def2-mTZVP) to obtain accurate geometries. Binding energies have been calculated by performing single point energy calculations at the most stable geometries (Fig. S12, S13). And the hydrogen bonding energy was then obtained by subtracting the energy of R- and S-CPA-Glu complex from the sum of glucose part and R/S-CPA part.

Enhancement factor. The enhancement factor (*EF*) can be calculated using the following equations:[7]

$$EF = (I_{SERS}/I_{bulk}) \times (N_{bulk}/N_{SERS}) \quad (1)$$

$$N_{SERS} = N_{MPBA} S_{Laser} \quad (2)$$

$$N_{bulk} = CVN_A S_{Laser}/S_{bulk} \quad (3)$$

where I_{SERS} and I_{bulk} are the vibration intensities in the SERS of 4-mercaptophenylboronic acid (MPBA) and normal Raman spectra of MPBA, respectively. N_{bulk} and N_{SERS} are the numbers of MPBA molecules under laser illumination for the bulk specimen, and the numbers of MPBA molecules on the GNRs, respectively. The number of MPBA molecules was calculated using equation (2) and (3), where C is the molar concentration of the MPBA solution, V is the volume of a droplet, N_A is the Avogadro constant (6.02×10^{23} mol^{-1}). S_{Laser} and S_{bulk} are laser spot size and the area of the MPBA solution dropped on the silicon wafer ($\pi\times (0.5/2)^2$ cm^2 = 0.196 cm^2). In the experiment, 10 μL of MPBA solution (0.2 M) was dried onto the Si wafer (d_{MPBA}=5 mm) and thus N_{bulk} can be estimated as:

$N_{bulk} = CVN_A S_{Laser}/S_{bulk}$ = [(10 μL×0.2 mol·L^{-1}×6.02×10^{23} mol^{-1})/0.196 cm^2] × S_{Laser}

$=6.1\times10^{10}$ μM^{-2}×S_{Laser}

N_{SERS} is determined by laser spot illuminating on the sample and density of MPBA molecule adsorbed on the surface of GNRs. According to the statistical data, the surface area of single GNR (S_{GNR}) is about 1260 nm^2 (60×21 nm^2=1260 nm^2). The surface area of the MPBA molecule (S_{MPBA}) is approximately 0.34 nm^2,[8] so the number of MPBA molecules adsorbed by one GNR is about 3706 [N_{MPBA}=1260/0.34=3706]. There are approximately 794 GNPs per square micron (N_{GNRs} = (1/1260) ×10^6 μM^{-2}=794 μM^{-2}), and thus N_{SERS} can be estimated as:

$$N_{SERS} = S_{Laser}\times 794\ \mu M^{-2}\times 3706 = 2.9\times10^6\ \mu M^{-2}\times S_{Laser}$$

I_{SERS} and I_{bulk} were obtained on the peak intensity of MPBA molecule at 1078 cm^{-1} in SERS spectrum in normal Raman spectrum as shown in Fig. S3, I_{SERS}=14688 and I_{bulk}=938. Substituting these values of into equation (1), EF can be calculated to be around 3.3×10^5 ([14688/938] × [6.1×10^{10}/ (2.9×10^6)] = 3.3×10^5).

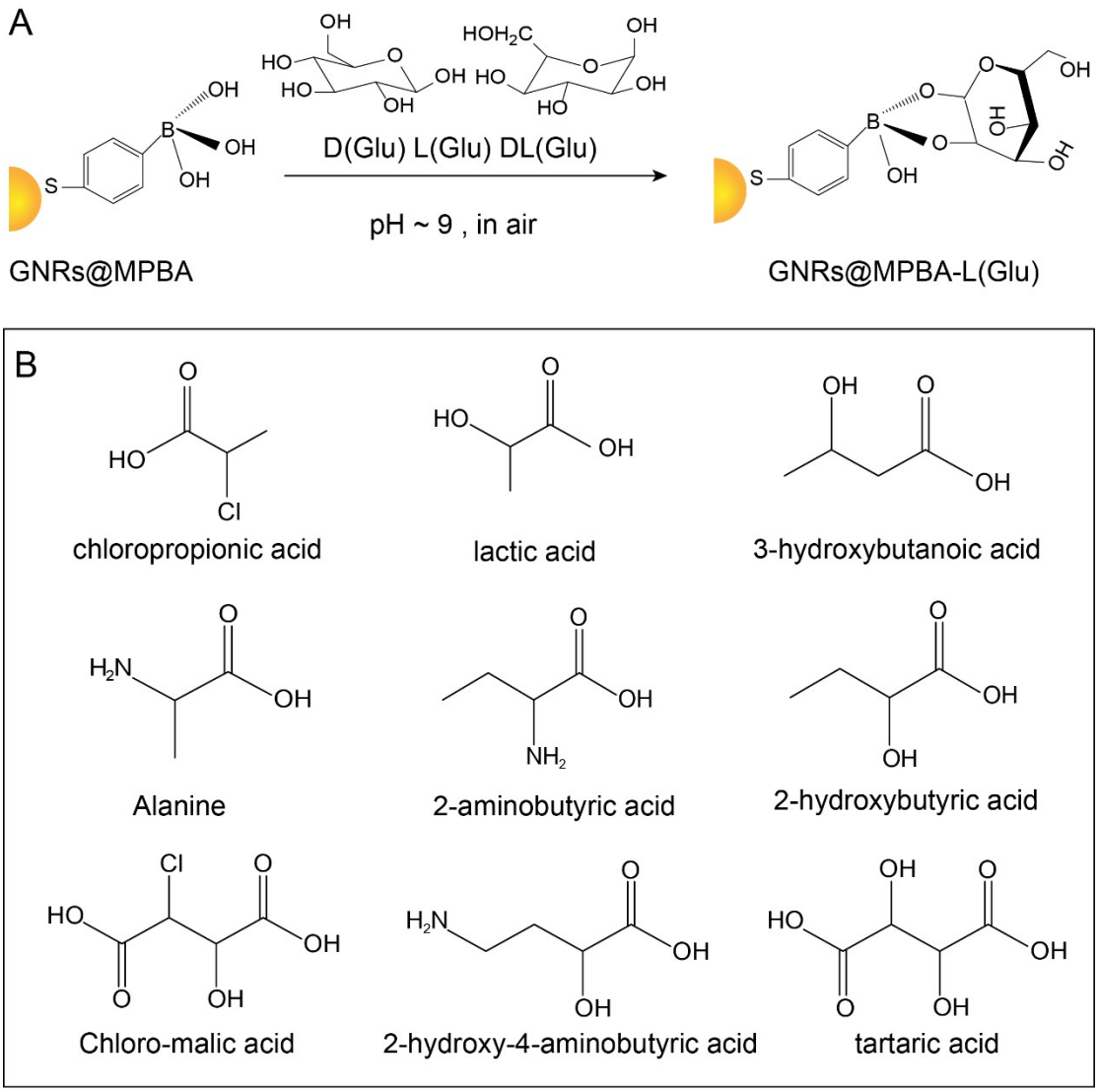

Scheme S1 (A) Schematic description of the molecular structures of chiral Glu and GNRs@MPBA, and the formation of chiral GNRs@MPBA-Glu. (B) Molecular structures of chloropropionic acid (CPA), lactic acid (LA), 3-hydroxybutyric acid (3HBA), alanine (ALA), 2-aminobutyric acid (ABA), 2-hydroxybutyric acid (2HBA), chloro-malic acid (CMA), 2-hydroxy-4-aminobutyric acid (HAA), and tartaric acid (TA).

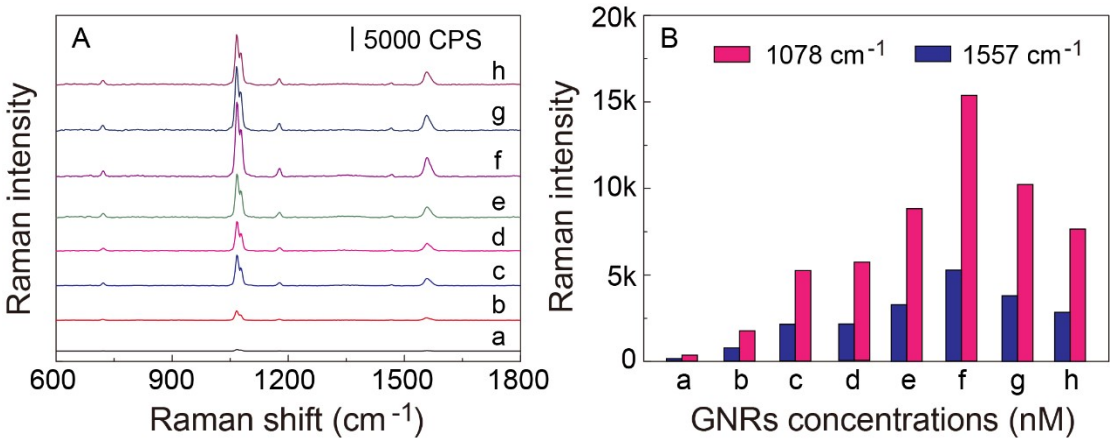

Fig. S1 (A) SERS spectra and (B) Raman intensities at 1078 and 1557 cm^{-1} of MPBA (10^{-4} M) on the surface of GNRs at different concentrations (a: 0.05, b: 0.1, c: 0.2, d: 0.3, e: 0.5, f: 0.6, g: 0.7, h: 1.0 nM).

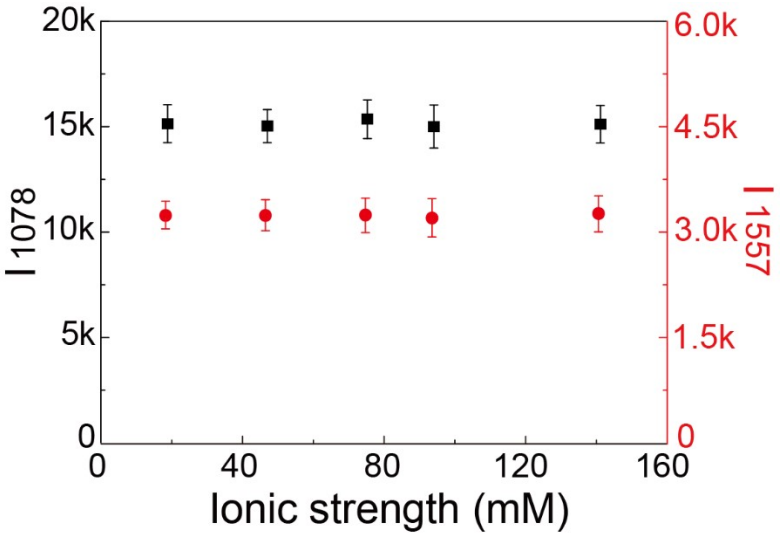

Fig. S2 The effects of ionic strength on Raman intensities at 1078 and 1557 cm^{-1} of MPBA (10^{-4} M) on the surface of GNRs. Each data point represents the average value from three measurements on the same samples. Error bars show the standard deviations.

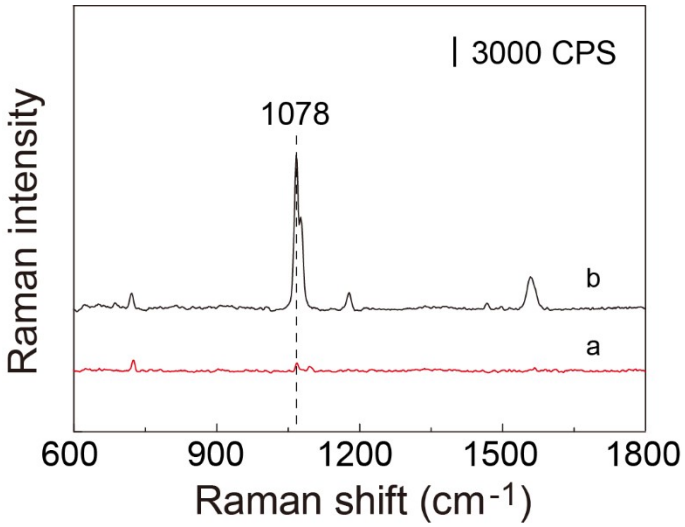

Fig. S3 (a) Normal Raman spectrum of 0.2 M MPBA. (b) SERS spectrum of MPBA (10^{-4} M) on the surface of GNRs.

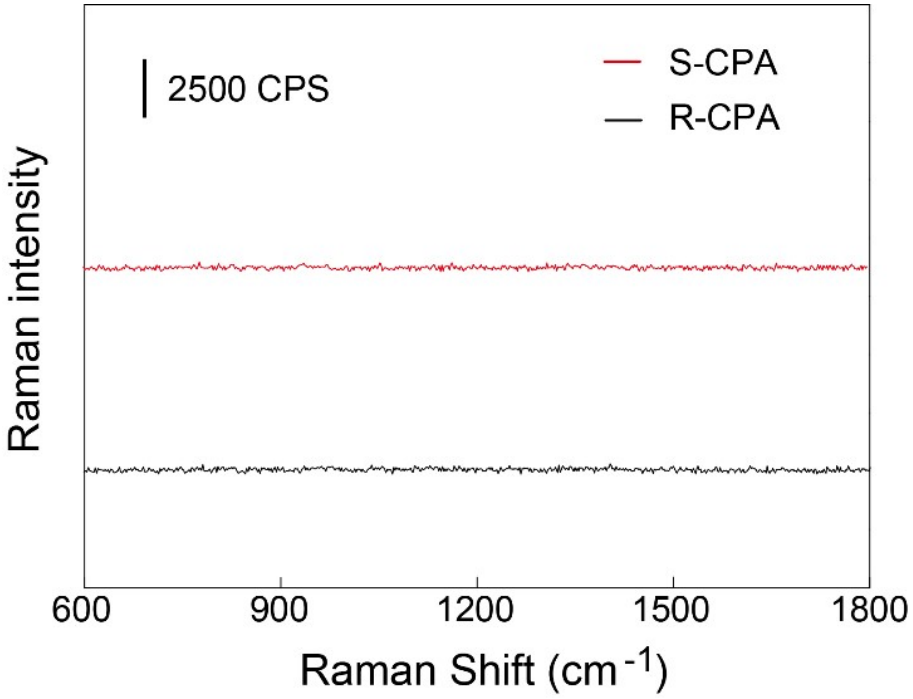

Fig. S4 Raman spectra for pure CPA enantiomers (black line for R-CPA and red line for S-CPA).

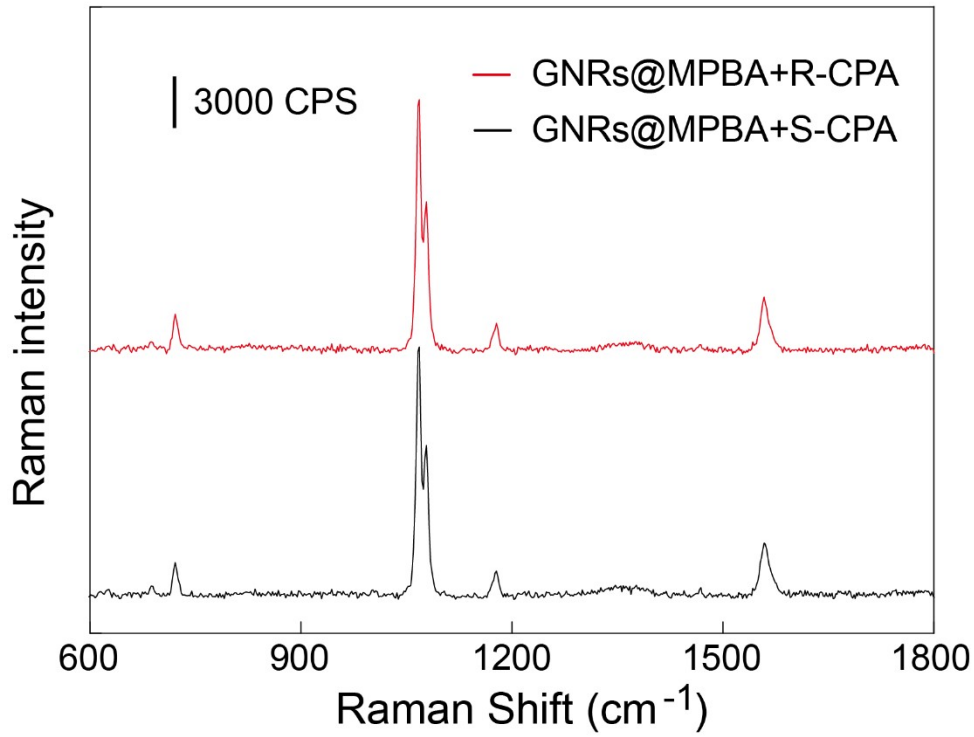

Fig. S5 SERS spectra of "GNRs@MPBA and S-CPA" (black line) and "GNRs@MPBA and R-CPA" (red line).

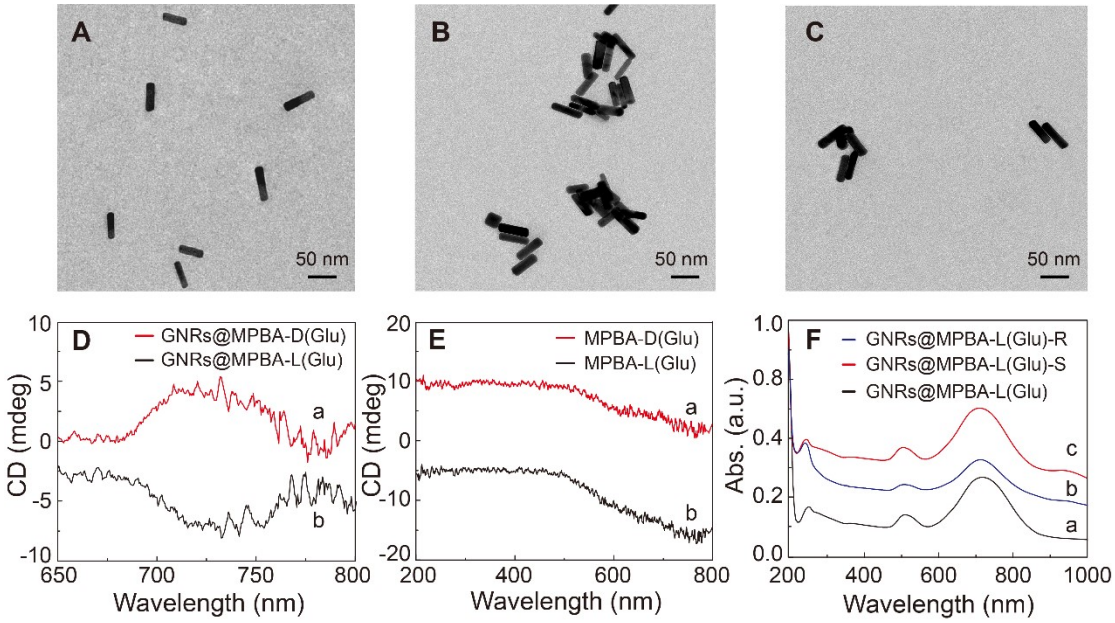

Fig. S6 TEM images of (A) GNRs@MPBA-L(Glu), (B) GNRs@MPBA-L(Glu)-S-CPA, (C) GNRs@MPBA-L(Glu)-R-CPA. CD spectra of (D): (a) GNRs@MPBA-D(Glu) and (b) GNRs@MPBA-L(Glu) and (E): (a) MPBA-D(Glu) and (b) MPBA-L (Glu). (F) UV-vis absorption spectra of (a) GNRs@MPBA-L(Glu), (b) GNRs@MPBA-L(Glu)-R-CPA and (c) GNRs@MPBA-L(Glu)-S-CPA.

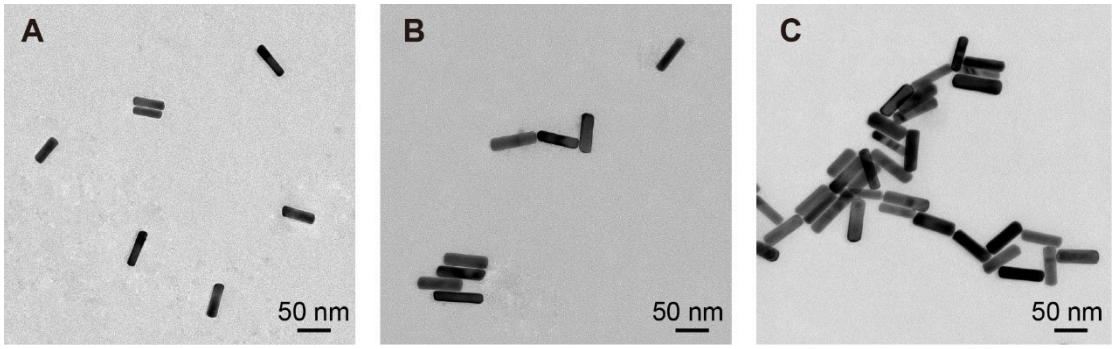

Fig. S7 TEM images of (A) GNRs@MPBA-D(Glu), (B) GNRs@MPBA-D(Glu)-S-CPA, (C) GNRs@MPBA-D(Glu)-R-CPA.

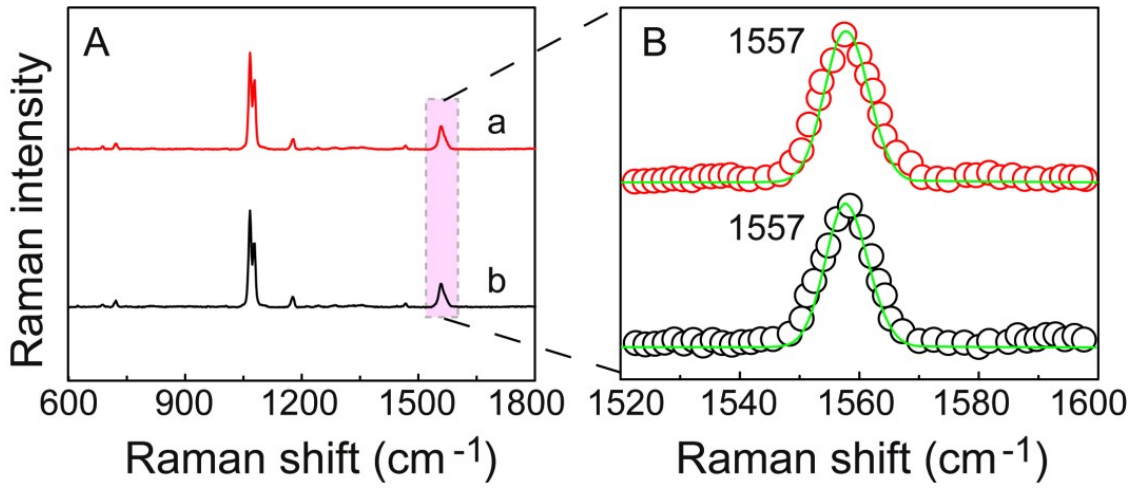

Fig. S8 SERS spectra of (A): (a) GNRs@MPBA-DL(Glu)-S-CPA and (b) GNRs@MPBA-DL(Glu)-R-CPA. (B) Enlargement of 1520-1600 cm^{-1} regions of SERS spectrum displayed in (A). All data was normalized to Raman signals at 1078 cm^{-1}.

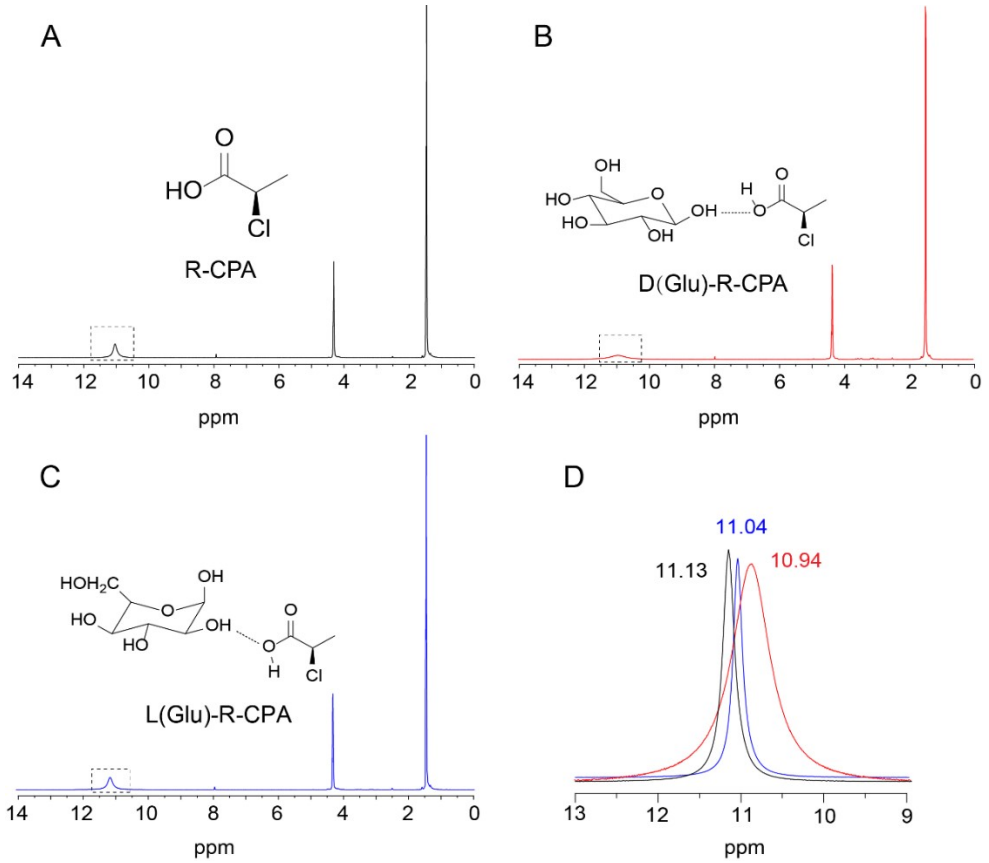

Fig. S9 ^{1}H-NMR spectra (500 MHz) of (A) R-CPA, (B) D(Glu) and R-CPA, (C) L(Glu) and R-CPA. (D) Partial ^{1}H NMR spectra from the (A-C).

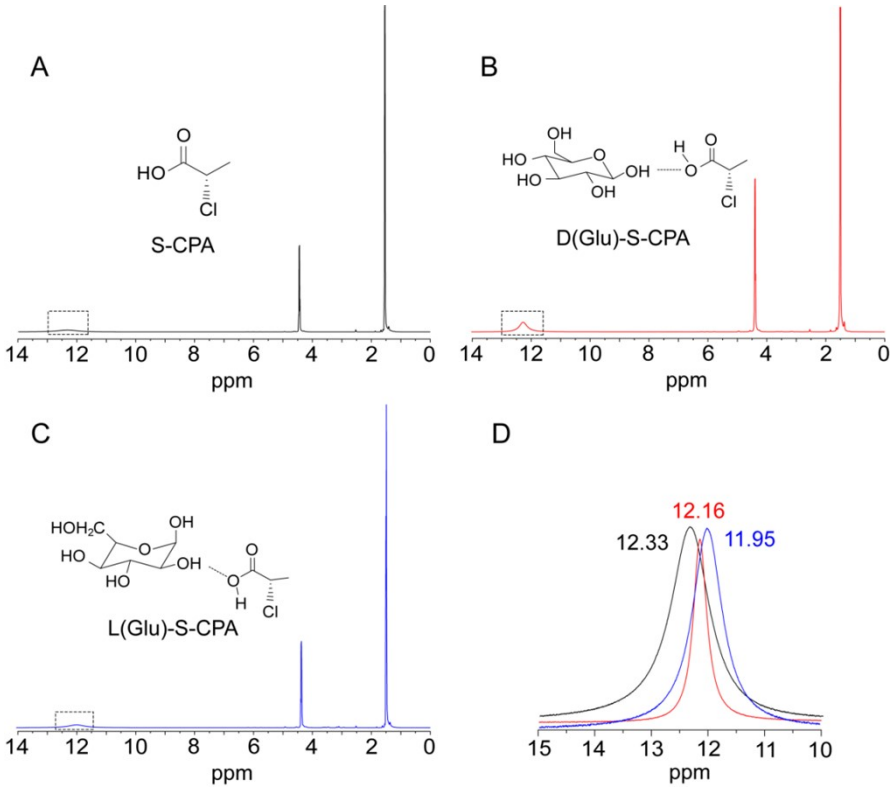

Fig. S10 ^{1}H-NMR spectra (500 MHz) of (A) S-CPA, (B) D(Glu) and S-CPA, (C) L(Glu) and S-CPA. (D) Partial ^{1}H NMR spectra from the (A-C).

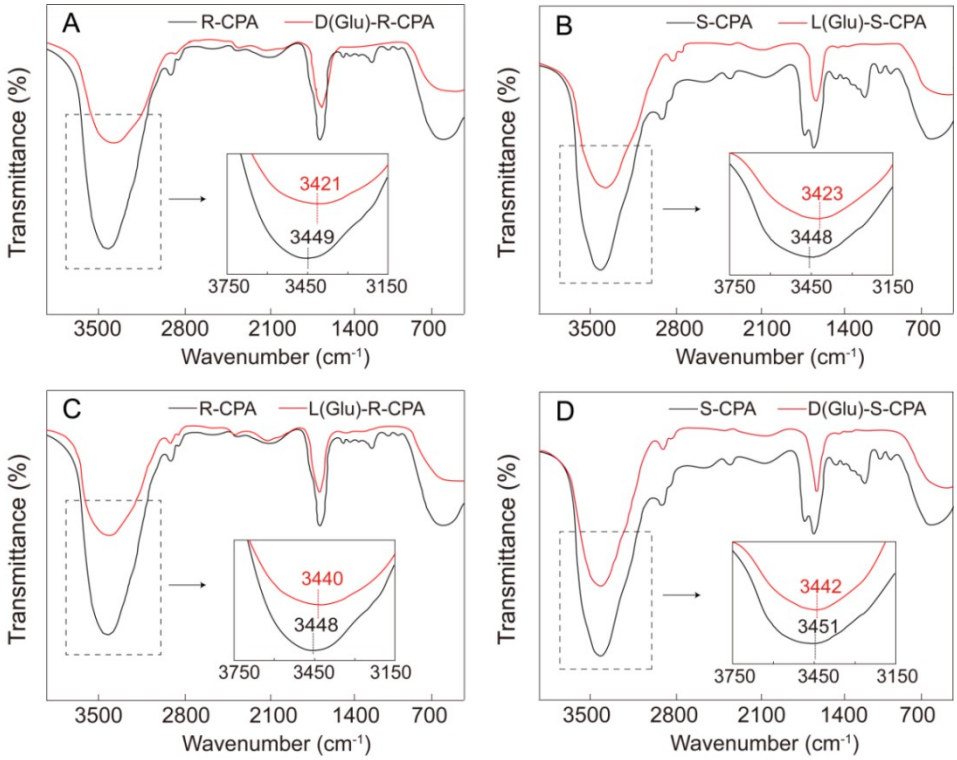

Fig. S11 FTIR spectra of the (A): R-CPA (black line) and D(Glu)-R-CPA (red line), (B) S-CPA (black line) and L(Glu)-S-CPA (red line), (C): R-CPA (black line) and L(Glu)-R-CPA (red line), (D): S-CPA (black line) and D(Glu)-S-CPA (red line).

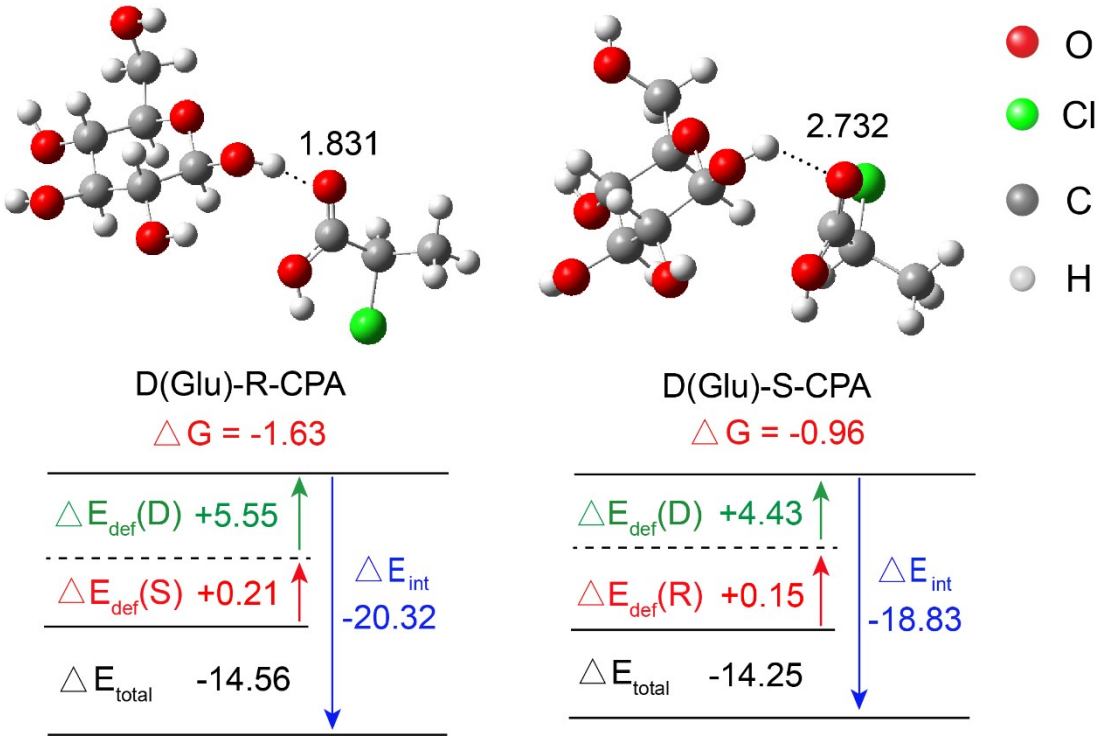

Fig. S12 Geometrical structures (distances in Å) of optimized species D(Glu)-R-CPA and D(Glu)-S-CPA.

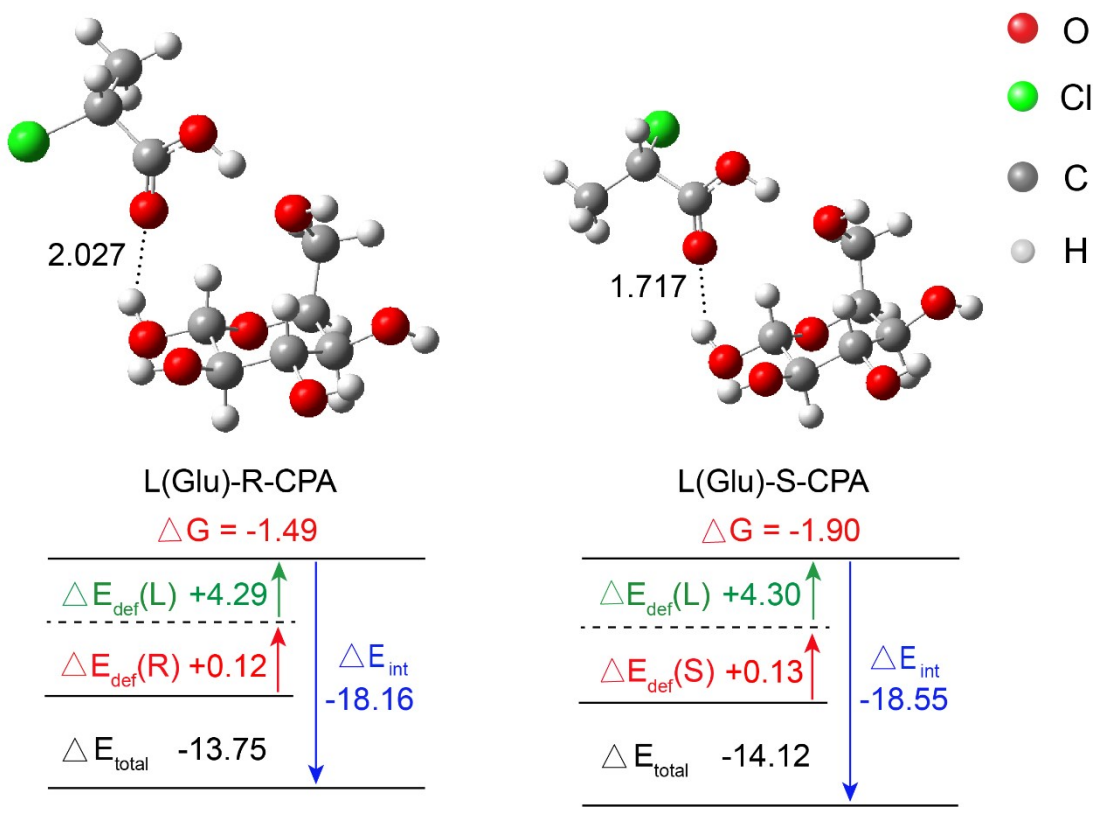

Fig. S13 Geometrical structures (distances in Å) of optimized species L(Glu)-R-CPA and L(Glu)-S-CPA.

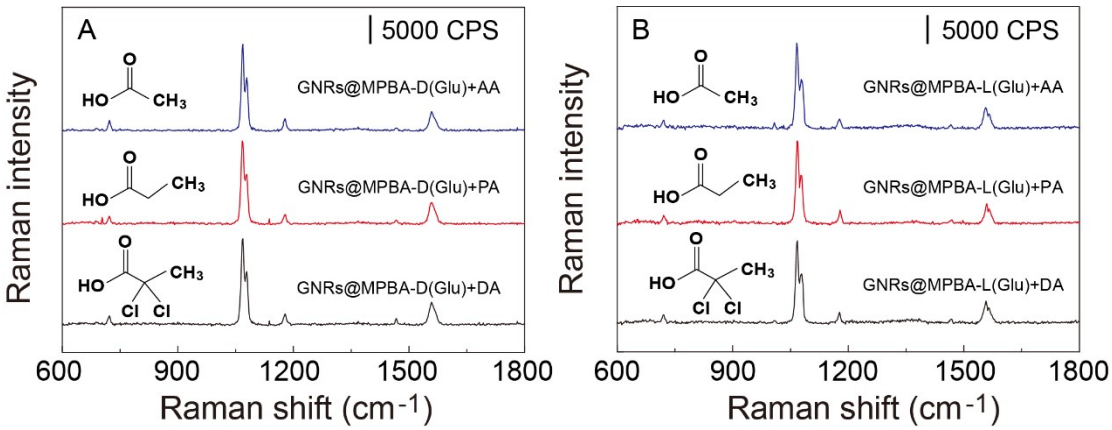

Fig. S14 SERS spectra of (A) GNRs@MPBA-D (Glu) and (B) GNRs@MPBA-L (Glu) in achiral chlorine-containing or chlorine-free carboxylic acids. From bottom to top: 2,2-dichloropropionic acid (DA), propanoic acid (PA) and acetic acid (AA).

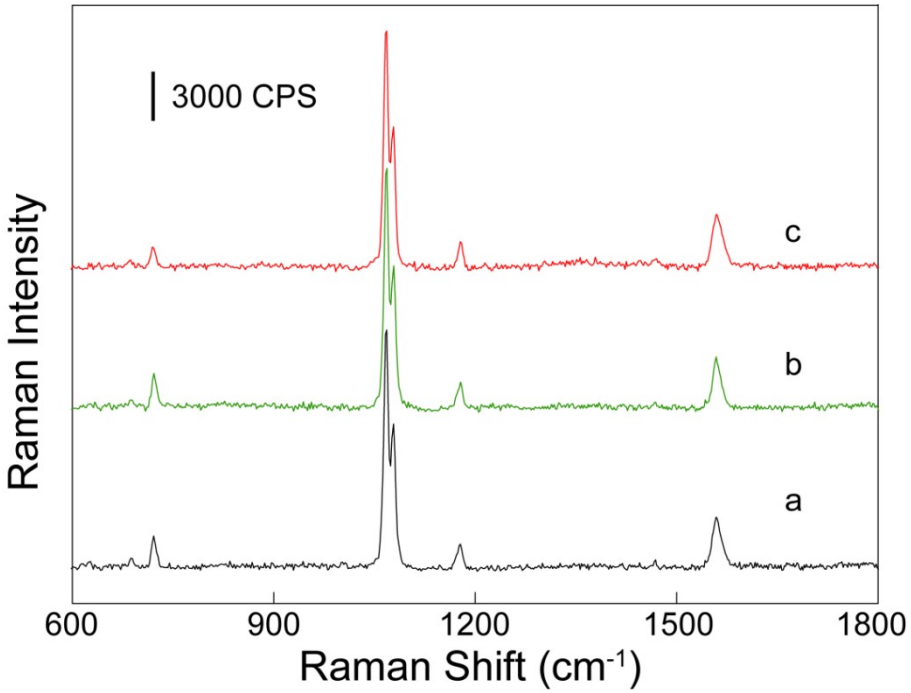

Fig. S15 SERS spectra of (a) GNRs@MPBA-PD, and the GNRs@MPBA-PD immersed in (b) R-CPA and (c) S-CPA. There is no difference between two spectra, indicating that the hydroxyl group is necessary for specific binding of CPA.

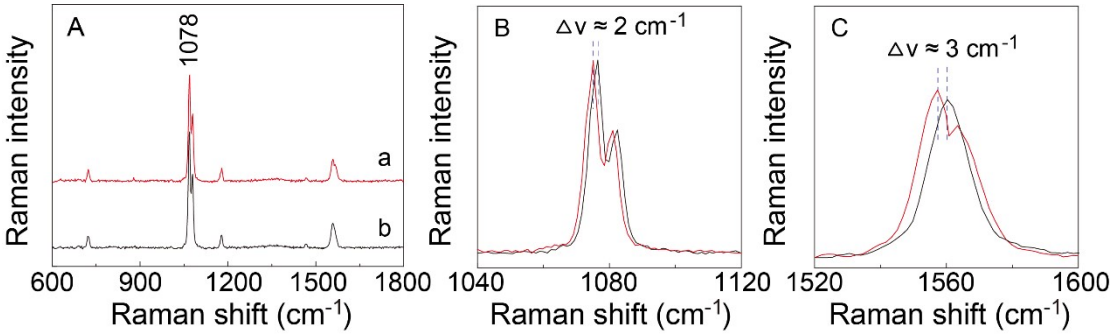

Fig. S16 (A) SERS spectra of the (a) GNRs@MPBA-L(Glu)-S-CPA and (b) GNRs@MPBA-L(Glu)-R-CPA, and expanded regions (B) 1040-1120 cm^{-1} and (C) 1520-1600 cm^{-1}. All the SERS spectra were normalized by the intensity of the band at 1078 cm^{-1}.

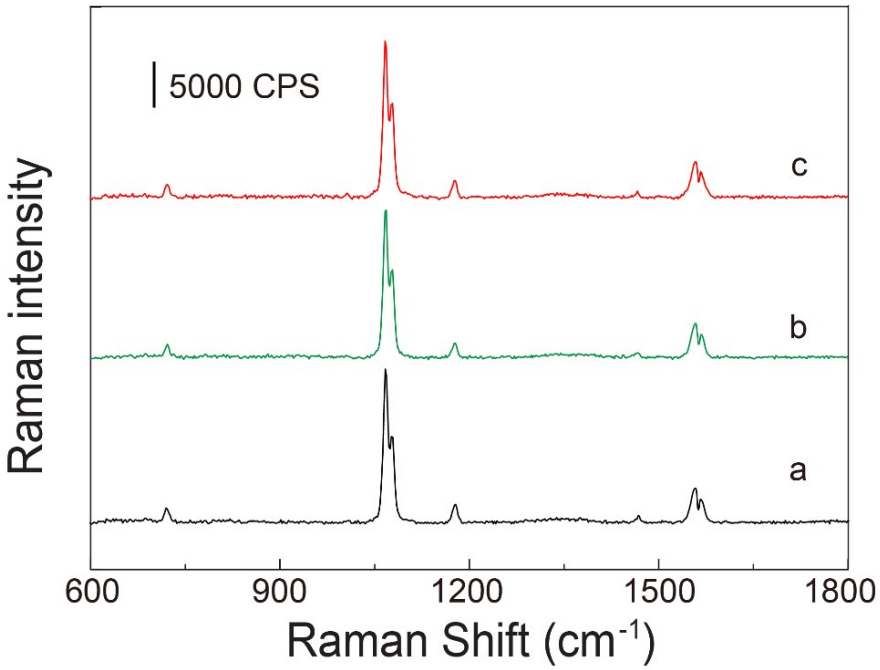

Fig. S17 SERS spectra of GNRs@3-MPBA-D (Glu) in blank solution (a), and GNRs@3-MPBA-D (Glu) in 10 mM R-CPA (b) or S-CPA (c) after incubation for 1 h. There is no significant difference among three spectra, indicating that the C_{2v} symmetry of the probe molecule is necessary for detecting CPA via symmetry breaking of the probe molecule upon CPA binding.

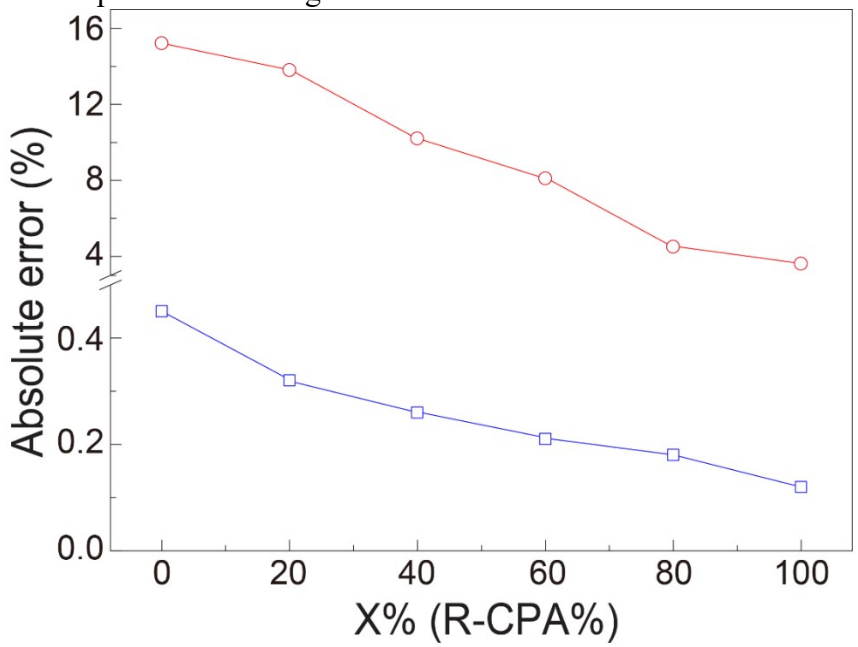

Fig. S18 Absolute errors of the various mass ratio of R-CPA evaluated by the PF-SERS method (blue square) and the absolute Raman intensity analysis (red circle). Error estimated from the average standard deviation of the calibration curve.

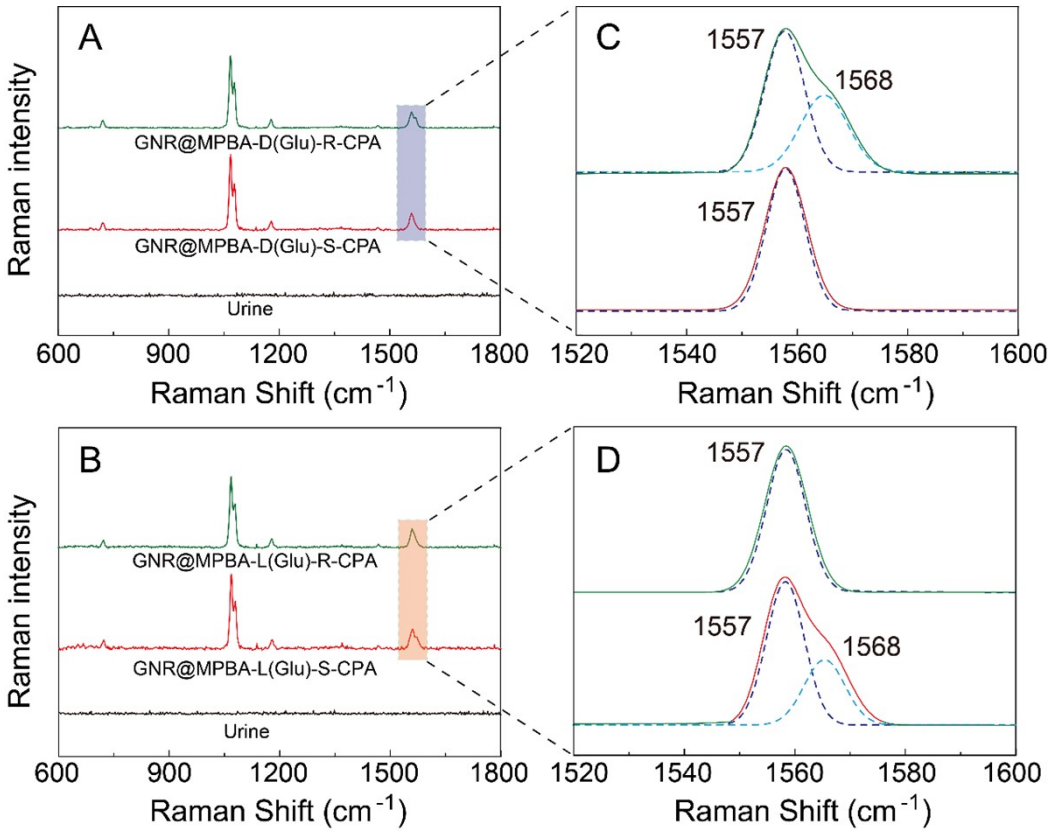

Fig. S19 SERS spectra of (A) GNRs@MPBA-D (Glu) and CPA, (B) GNRs@MPBA-L (Glu) and CPA (the red lines for the mixtures containing S-CPA while the green ones for R-CPA). Raman spectra of urine (black line) spiked with R-CPA and S-CPA. (C, D) Enlargement of 1520-1600 cm^{-1} regions of SERS spectrum displayed in (A, B). All data was normalized to Raman signals at 1078 cm^{-1}.

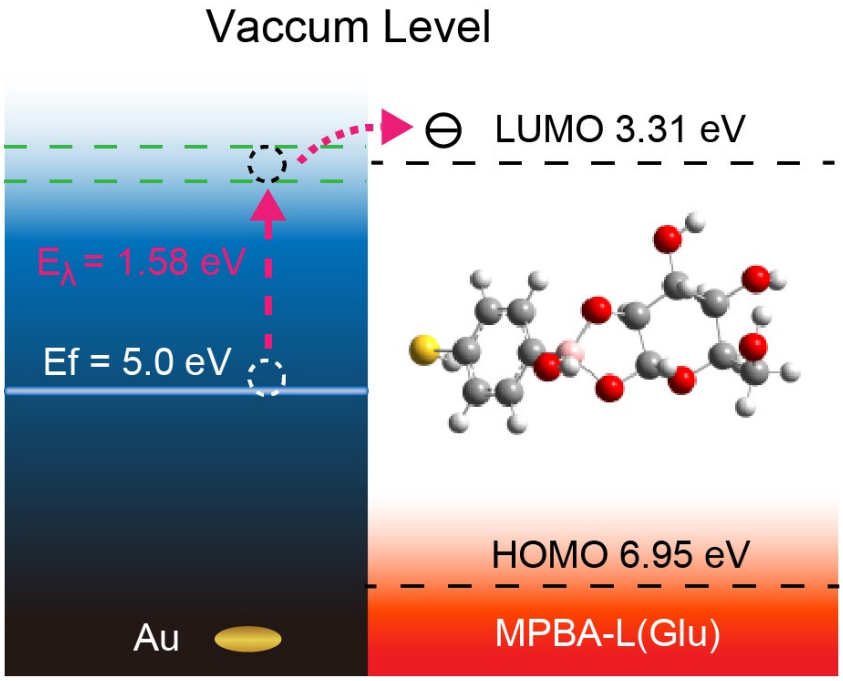

Fig. S20 Energy level diagram of the Au@MPBA-L(Glu) complex assembly at the energy of the 785 nm laser excitation.

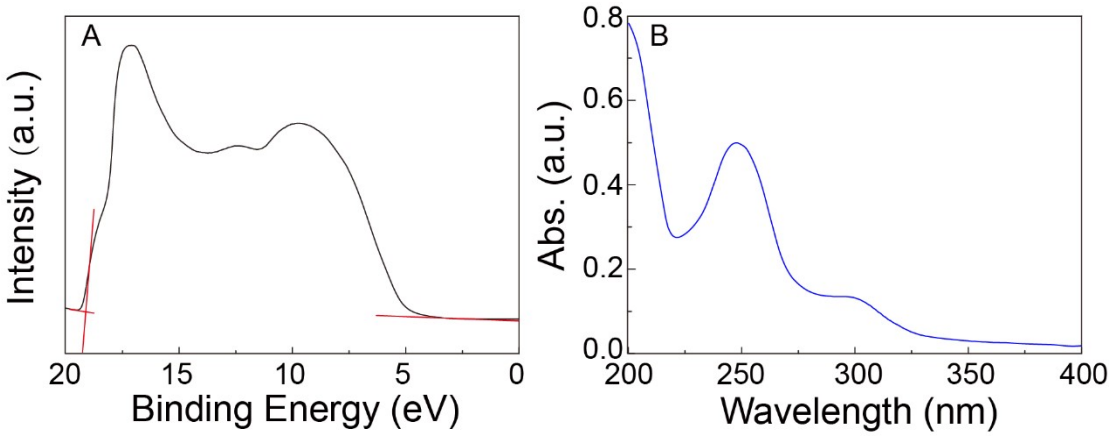

Fig. S21 (A) UPS spectrum of GNRs@MPBA-L(Glu). (B) UV-vis absorbance spectrum of MPBA-L(Glu) in ethanol.

Table S1 Raman and SERS Vibrational Frequencies for MPBA [9]

Raman (cm^{-1})	SERS (cm^{-1})	Assignment [a]
631	626	ν_{CS}
722	726	4b; γ_{CCC}
907	907	β_{CSH}
1092	1078	1; $\beta_{CCC}+\nu_{CS}$
1102	1098	15; β_{CH}
1187	1176	9a; $\beta_{CH}+\beta_{BOH}$
1595	1557	8b; ν_{CC}
	1568	8a; ν_{CC}

[a] ν; stretching, β; in plane bending, γ; out of plane bending

Table S2 RSD values for different substrates and the DI of the three types of GNRs@MPBA-Glu toward CPA enantiomers

Substrate	RSD		Comparing A_S and A_R	DI
	S-CPA(%)	R-CPA(%)		
GNRs@MPBA-L(Glu)	3.51	6.15	$A_S > A_R$	1.6
GNRs@MPBA-D(Glu)	6.97	3.07	$A_S < A_R$	1.2
GNRs@MPBA-DL(Glu)	4.53	5.31	$A_S \approx A_R$	1.0

Table S3 Comparison of performance of PF-SERS method and HPLC method for determination of R-CPA with various mass ratios (n=3).

Samples (R-CPA%)	PF-SERS		HPLC	
	Calculated (%)	RSD (%)	Calculated (%)	RSD (%)
100	96.7	2.8	99.3	1.6
80	83.5	3.5	80.1	1.8
60	65.2	2.9	61.5	2.3
40	37.8	3.2	39.1	1.9
20	18.6	4.1	21.6	2.5
0	0.18	2.1	0.05	1.3

References

[1] Z. Xia, D. Li, and W. Deng, *Anal. Chem.* 2021, **93**, 4924-4931.

[2] C. J. Orendorff and C. J. Murphy, *J. Phys. Chem. B* 2006, **110**, 3990-3994.

[3] F. Neese, *WIREs Comput. Mol. Sci.* 2018, **8**, e1327.

[4] J. G. Brandenburg, C. Bannwarth, A. Hansen and S. Grimme, *J. Chem. Phys.* 2018, **148**, 064104.

[5] A. D.Becke, J. Chem. Phys. 1997, 107, 8554-8560.

[6] S. Grimme, S. Ehrlich and L. Goerigk, *J. Comput. Chem.* 2011, **32**, 1456-1465.

[7] X. Yue, Y. Su, X. Wang, L. Li, W. Ji and Y. Ozaki. *ACS Sens.* 2019, **4**, 2336-2342.

[8] Y. C. Kao, X. Han, Y. H. Lee, H. K. Lee, G. C. Phan-Quang, C. L. Lay, H. Y. F. Sim, V. J. X. Phua, L. S. Ng, C. W. Ku, T. C. Tan, I. Y. Phang, N. S. Tan and X. Y. Ling, *ACS Nano* 2020, **14**, 2542-2552.

[9] K. Whang, J. Chang, K. Jung, H. Ko, J. Lee, I. Choi and T. Kang, *Anal. Chem.* 2019, **91**, 13152-13157.